Semiconductor Manufacturing Process Optimisation

Said Kafumbe
Electrical Engineering Technology
Higher Colleges of Technology
Abu Dhabi, UAE

***Abstract*— In a semiconductor manufacturing process the number of process steps as well as the time taken by each step are vital in determining the yield and volume of the manufactured device. Additionally, the manufacturing recipe used at each process greatly determines the reliability and performance of the finished design. By tweaking the process recipe as well as the process times an optimized manufacturing process can be obtained. This work presents process optimization at both the electroplating, cmp and plasma ashing steps for various semiconductor devices with improved performance for all devices.**

Keywords— engineering; mathematics; examples; and problems;

I. INTRODUCTION

The manufacturing yield in semiconductor devices is affected by many factors [1-3]. These are mainly related to the variations that occur within each process step that are beyond control. The number of materials involved in the process each having different characteristics as well as the uncontrollable effects of the equipment involved in the manufacturing process are bound to result in process variations. Human factors in the handling of the manufactured devices from one process step to another are also sources of unintended errors which result in the effect to the quality, quality as well as the reliability and performance of the finished devices. All these uncontrollable factors occurring within the manufacturing process prompt novel ways of tweaking and optimizing the semiconductor manufacturing process to improve the reliability, production volume as well as yield of the manufactured devices thus lowering the scrap quantity. This not only lowers production costs but it decreases the number of reruns of the same manufacturing process.

Optimization of the manufacturing process has been done before using a control framework based on technology transitions [1-2]. Additionally, the use of virtual predictions has been employed in process control [3-5]. However for in situ optimization of the manufacturing process, direct wafer by wafer monitoring and control through tweaking of process parameters and recipe results in a more efficient and versatile manufacturing process as well as improved yield.

In this work, both the electroplating, cmp as well as the plasma ashing process steps were optimized in a number of reruns to enhance yield of a MEMS cantilever array and a metal insulator metal capacitor shown in figure 1.

II. METHODOLOGY

A. Electroplating process

The electroplating process was carried out for the fabrication of the vibrating structure of the cantilever beam made of gold material. In this work, the electroplating was used to deposit Au thickness of 2μm in a thiosulfate-sulfite bath and process started with the calculation of the plating area. Sketches of the structure after electroplating are shown in Fig. 15, and those after photoresist was completely removed, in Fig. 16. This key parameter dictates the final thickness of the plated material (Schlesinger, M., 2010). The exposed area for electroplating was 5.6 cm2. Using the atomic mass of Au of 196.67 g/mole, and a density of 19.3 g cm-3, an area of 5.6 cm2 with a plating current of 11 mA, would take approximately 20 minutes to deposit 2μm of Au.

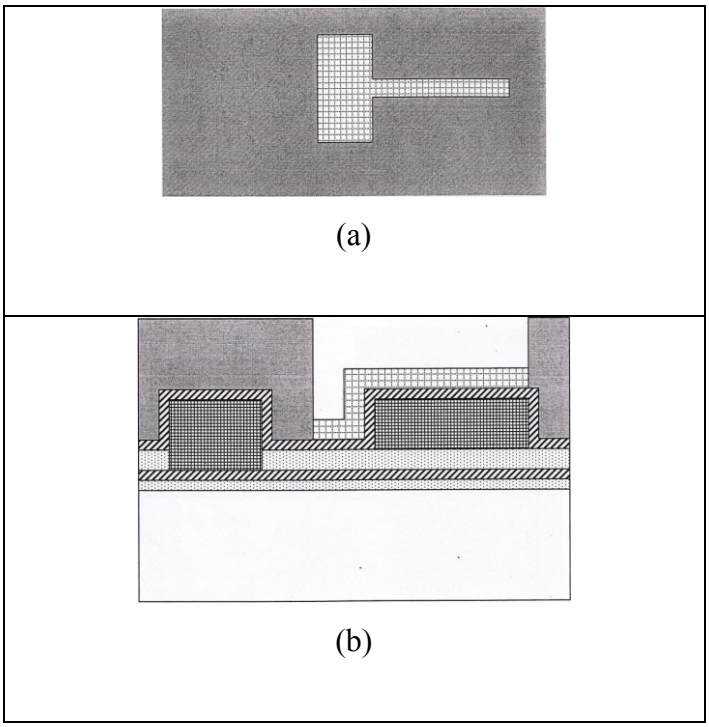

(a)

(b)

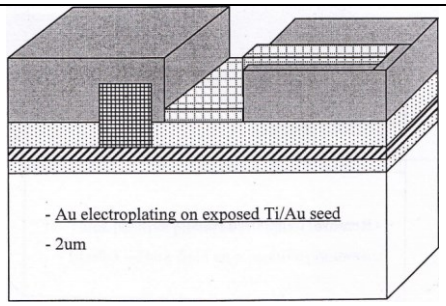

(c)

Fig. 1. Au electroplating to a thickness of 2µm on exposed parts of the seed layer deposition: (a) top view; (b) side view; (c) 3-D view

A low power oxygen plasma clean, also called a descum, was done to remove any remaining resist residues on the wafer that might be covering the area to be plated. The wafers were then weighed, rinsed and dried ready for plating. The plating system, based on a thiosulfate-sulfite bath, consisted of the following components: vertically mounted Perspex (polymethyl methacrylate) flow channel, a polypropylene plating reservoir equipped with a poly (tetrafluoroethylene) encased heater, a magnetically coupled pump, and a filter chamber. The various components were connected using polypropylene piping and the flow was controlled via a network of pneumatically controlled valves. A flow rate of 175 ml/s was used, and this corresponded to a turbulent flow regime.

The solution was continuously filtered through a pair of 1µm retention polypropylene filters to remove particulates. The electrodeposition experiments were performed under constant current conditions using a computer-controlled direct current power supply (Zareian-Jahromi, M.A. and Agah, M. 2009). The flow rate was measured using an in-line paddle rotameter, and the temperature in the flow channel was measured via a calibrated thermocouple. Wafers were plated in a vertical flow channel.

In the implementation of this step, the wafer was mounted on one wall of the channel and a 100mm wide Au plate-mesh anode mounted on the opposite wall. The anode dissolved under the influence of the plating current; forming gold ions that replace those discharged thus depositing as metallic gold on the wafer which acts as the cathode. The gap between the anode and wafer cathode was 1 cm, and the width of the channel was 12cm. The wafer sat flush with the channel wall, and the electrical contact was made via four insulated probes which contacted the front side of the wafer near the periphery.

The electroplating solution used was a ready-to-use gold electroplating solution ECF60 (sulphide gold) with a concentration of 10 g/l, and a pH of 9.4. It was allowed to circulate for 3 minutes prior to plating so as to allow sufficient time for thermal equilibration and to dislodge any air bubbles that may be trapped in the resist pattern. After this time, a current corresponding to the desired deposition rate was applied. A current density of 1.96 mA/cm2 was used in the deposition. To ensure that the plating bath is homogeneously at 50oC, a magnetic stirrer was used. This helped in achieving good uniformity and delivering reactants from the bulk solution to the regions near the cathode. Other parameters used in the electroplating process included a plating voltage of 0.97V, current of 11mA, a flow rate of 170ML/s, and a plating time of 20s. These parameters were varied for different runs aimed at achieving an approximate thickness of 2µm.

After plating, the wafers were rinsed, dried and then weighed. The patterning photoresist was then removed with a commercial resist stripper (acetone), and the Au deposited measured. The average weight of the deposited gold was measured as 29.47±4.43µm while the average gold thickness before and after removal of the Ti/Au seed layer was 2.10±0.05µm and 2.04±0.05µm respectively. From these measurements, it is clear that the final etch of the seed layer does remove part of the beam material. Although it is important that the entire seed layer is etched away, care has to be taken to avoid reducing the beam thickness significantly. The surface roughness (measured using a surface profilometer) of the plated gold was 125Å, which compares well with previous values of 200–250nm (Green, T. A. et al, 2003). Surface roughness plays no particular importance in this work, but flat surfaces improve the reflection of the laser beams from a laser Doppler vibrometer during frequency tuning testing of the device.

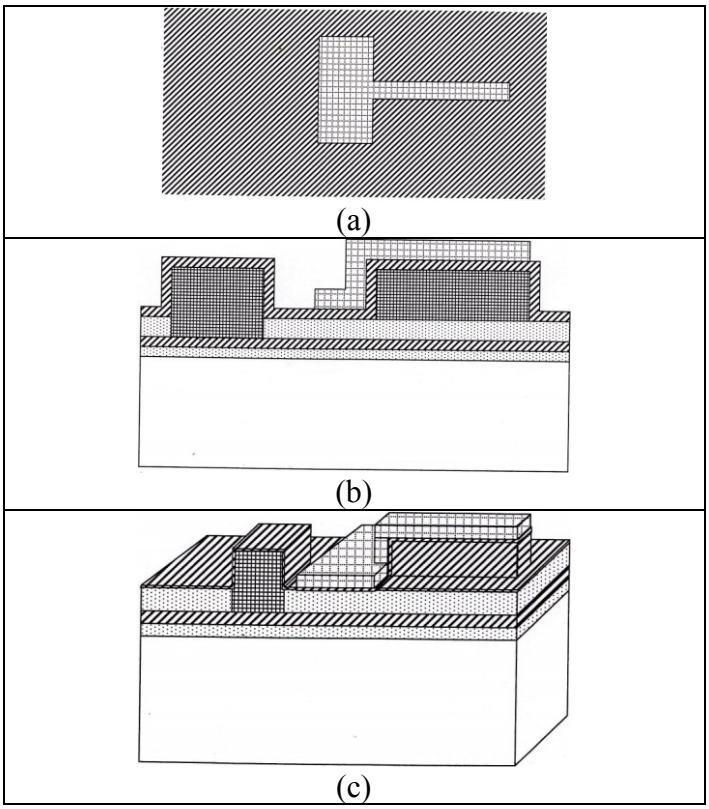

(a)

(b)

(c)

Fig. 2. Photoresist strip exposing electroplated Au and Ti/Au seed layer: (a) top view; (b) side view; (c) 3-D view

B. Plasma ashing

The electroplated gold beam structures were released by completely etching away the photoresist sacrificial layer in an oxygen (O2) plasma asher using end-point detection and over etch technique (Bartek, M. and Wolffenbuttel R. F., 1998). The sketches of this step are shown in Fig. 19. During the process, the flow rate of O2 was set at 800 ml/min, the chamber pressure at ~1mbar, and the microwave power at 500W.

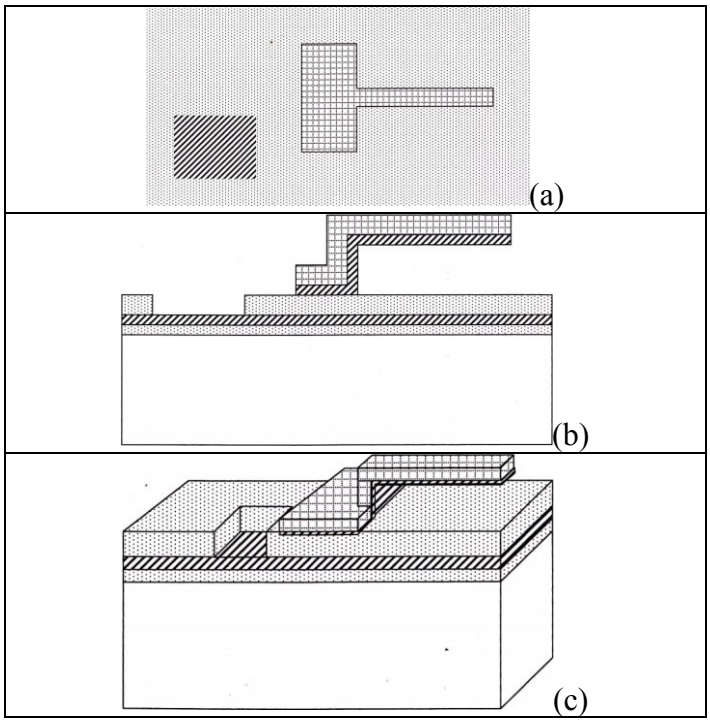

Fig. 19. Oxygen plasma ashing of regions covered by photoresist to release the cantilever: (a) top view; (b) side view; (c) 3-D view

To avoid carbonizing the photo-resist, the chamber temperature was set not to exceed 150oC since continuous heating of the devices may cause a higher rise in average temperature (Chatzandroulis, S., et al, 2002). Due to the different thermal expansion coefficients between the metallic films, unwanted differential stress may result and cause irreversible deformation. This is especially true if the strain incurred goes beyond the elastic limit of the metallic film well into the plastic regime. The ashing time was controlled to avoid inducing thermal stresses that will deform the beam after release (Mastrangelo, C. H., 1993). Ashing was carried out for 6.5 minutes using a 500W plasma and for 12 minutes using a 250 W plasma. Fig. 20 shows released cantilevers.

C. Metal insulator metal capacitor

Nevertheless, the examples and problems were reviewed and collected for reference. The data from these courses could also be used in the future part of this work where examples and problems from lower semester courses could be used in higher semester courses that are within the same in the same hierarchy and are prerequisites for them.

III. Results and Discussion

The XL30 ESEM-FEG scanning electron microscope (SEM) was used to closely inspect the released devices, to measure the cantilever thickness as well as the separation gap between the cantilever and the insulated substrate with a resolution of 2nm (Griffin, N. S., 1994). This was done progressively as the release process was being optimized to obtain relatively flat cantilever beams. Initially, released beams were bent upwards due to residual stress as shown in Fig. 23. These devices were released with a plasma power of 500W after 12 minutes of oxygen ashing.

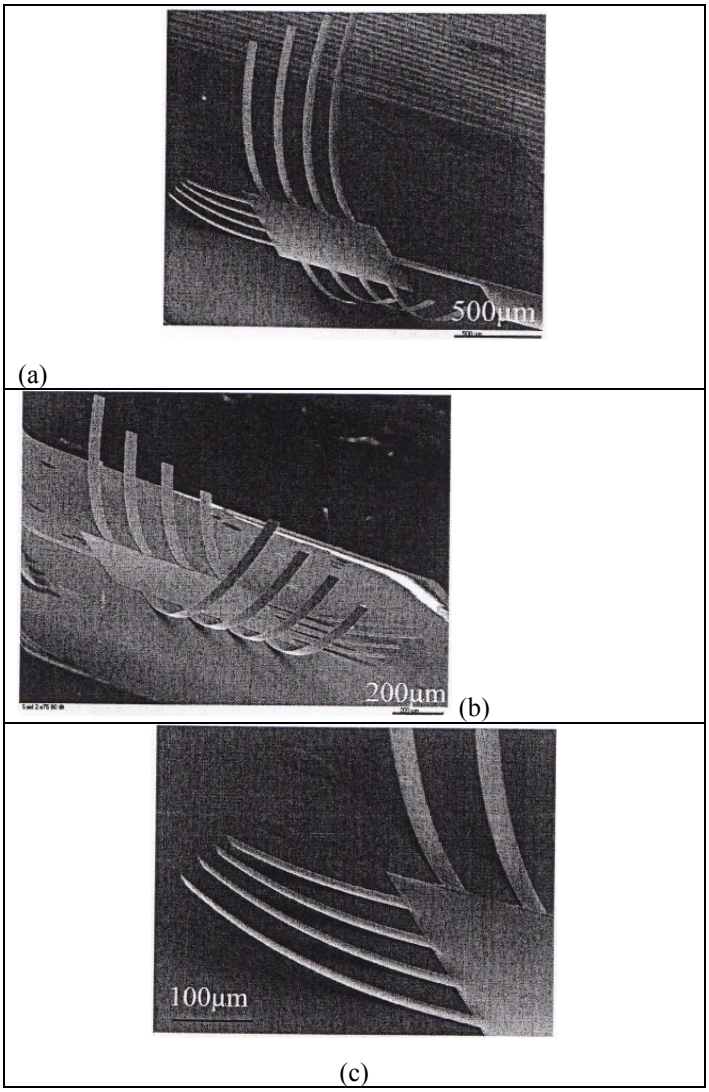

Fig. 3. SEM images of the suspended beams before the oxygen plasma ashing power was optimised: (a) all beams wide view; (b) close up view of the longer beams; (c) close-up view of the shorter beams

After lowering the oxygen plasma power to 250W, and the ashing release time to 7.5 minutes, flat beams were observed as shown in Fig. 24. To analyse the gap between the beams and the substrate, close-up views of the beam tips and sides were taken as shown in Fig. 25. Additionally, the thickness of the beam was measured as shown in Fig. 26.

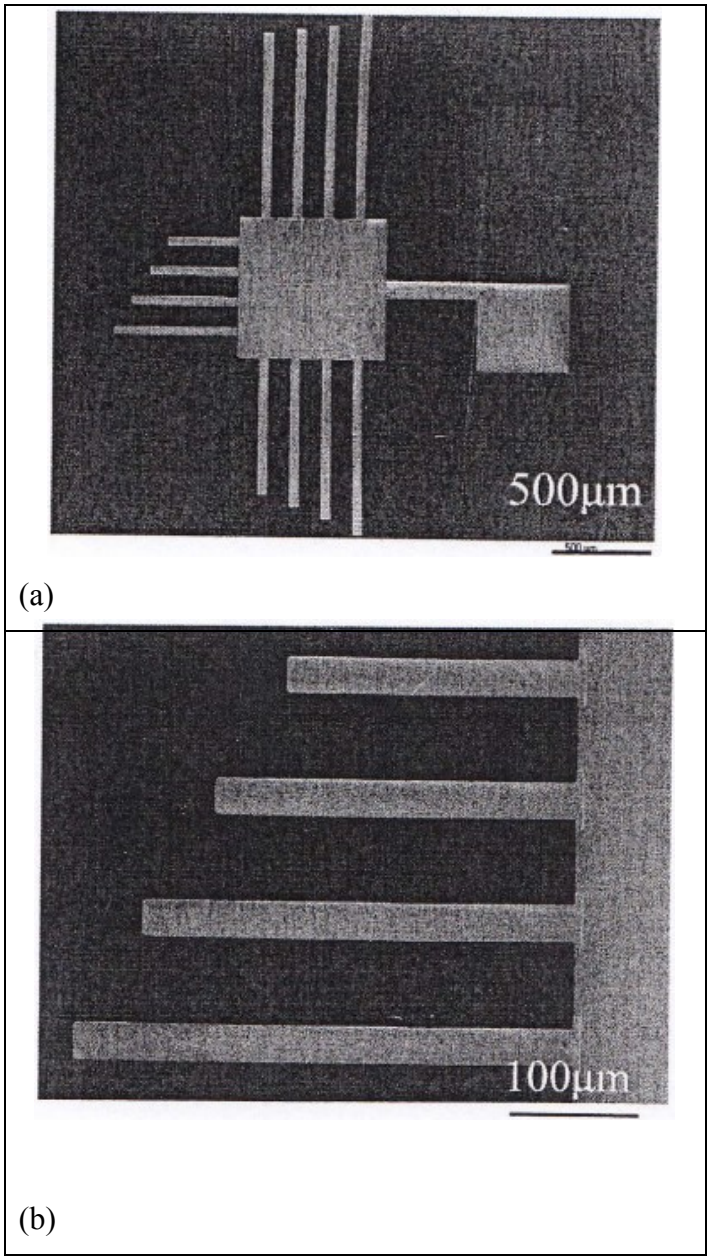

Fig. 4. SEM images of the flat beams after optimising the plasma ashing process: (a) all beams wide view; (b) close-up view of the shorter beams

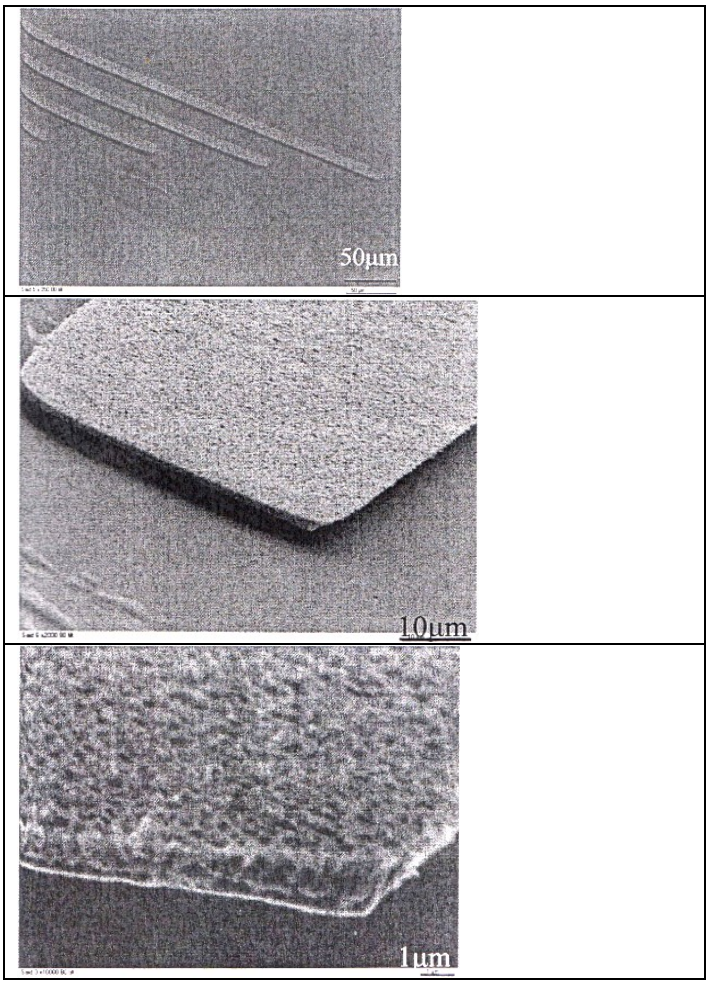

Fig. 5. SEM images of the flat beams after optimising the plasma ashing process: (a) some of the longer beams wide view; (b) close-up view of the beam; (c) a much closer view of the beam for thickness measurement

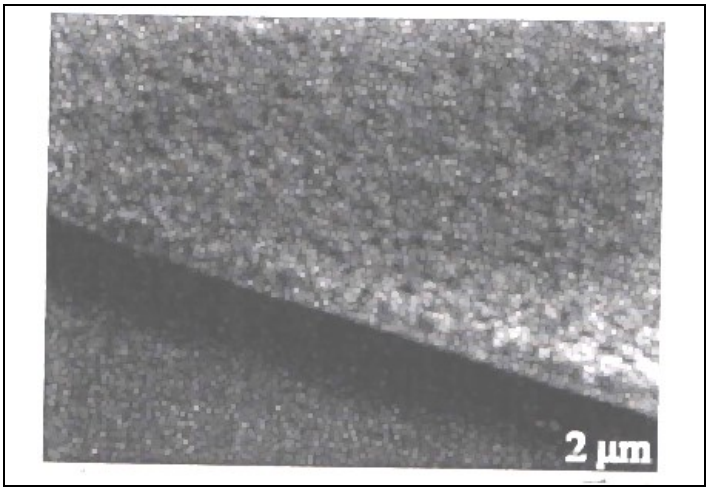

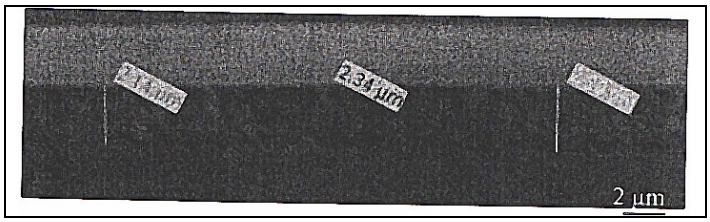

Fig. 6. SEM images of the flat beams after optimising the plasma ashing process: (a) some of the longer beams wide view; (b) close-up view of the beam; (c) a much closer view of the beam for thickness measurement

From the results shown in the preceding paragraphs, it is evident that initially, the released beams were not ideally flat. The end-tip was bent upwards with the initial deflection increasing with the length of the beam as shown in Fig. 23. This bending was attributed to several factors: firstly the high temperatures that are involved in the oxygen ashing process introduced thermal stresses. These temperatures depended on the oxygen plasma power and the duration of the ashing process. As the device was removed from the asher, the difference in temperature causes the beam tip to bend since the other end is fixed. Secondly, there could have been a deposition tensile stress due to the electroplating bath. This is because several wafers based on different processes were used in the same plating bath as this work. These wafers might have introduced impurities in the plating solution that resulted in a change in the stress of the deposited Au film. Other factors that could have resulted in a change in the stress include: the bath life and aging of the plating solution; plating without additives, accelerators and suppressors in the solution that should have increased plating throwing power and uniformity; and not annealing the device after plating. Additionally, the upward bending could also be attributed to the thermal mismatch between the thin Ti metal underneath the Au seed layer, and the electroplated Au.

On the whole, the deflection of the released cantilever beams was dependent on the dry-release ashing process time, and it was concluded that thermal stress was incurred during the plasma etching process. Since this additional stress can be inconclusively distinguished from the deposition stress, the post-deposition process such as a dry-release method also needs to be controlled for accurate characterization. Several solutions might be available including the use of a bridge (fixed-fixed) beam configuration to cancel the stresses. An immediate solution, which was employed in this work was to change the ashing process recipe to allow for low plasma power and intermittent ashing. Results show that an optimum ashing time can be reached where the beams are almost entirely flat. These are shown in Fig. 24 and Fig. 25. No stiction was observed in the cantilevers.

IV. Conclusions and Future Work

Sample examples and problems borrowed from engineering were generated that could be used in teaching and learning of mathematics courses to enable students understand and apply what they learn in engineering and while at the same time seeing the relevancy of the courses. The key criteria however was to consider that mathematics and engineering courses that are taught in the same semester or level were mapped together so that examples and problems from the engineering courses at that level or semester where the ones used in the mathematics courses at that level or semester. To generate sample examples and problems, text books, course outlines, as well as electronic archives of the courses, were used. It was found that specific topics in mathematics courses matched those in engineering courses at the same level or semester, and examples or problems could be easily integrated and used during teaching and learning.

Other courses that are not related to mathematics would also benefit from this novel technique where students apply what they learn on one side as they do another course. This is the focus of further work.

References

[1] Qin, S.J., Cherry, G., Good, R., Wang, J. and Harrison, C.A., 2006. Semiconductor manufacturing process control and monitoring: A fab-wide framework. Journal of Process Control, 16(3), pp.179-191.

[2] Qin, S.J., Cherry, G., Good, R., Wang, J. and Harrison, C.A., 2004. Control and monitoring of semiconductor manufacturing processes: Challenges and opportunities. IFAC Proceedings Volumes, 37(9), pp.125-136.

[3] Chen, P., Wu, S., Lin, J., Ko, F., Lo, H., Wang, J., Yu, C.H. and Liang, M., 2005, September. Virtual metrology: A solution for wafer to wafer advanced process control. In Semiconductor Manufacturing, 2005. ISSM 2005, IEEE International Symposium on (pp. 155-157). IEEE.

[4] Khan, A.A., Moyne, J.R. and Tilbury, D.M., 2007. An approach for factory-wide control utilizing virtual metrology. IEEE Transactions on semiconductor Manufacturing, 20(4), pp.364-375.

[5] Kang, P., Kim, D., Lee, H.J., Doh, S. and Cho, S., 2011. Virtual metrology for run-to-run control in semiconductor manufacturing. Expert Systems with Applications, 38(3), pp.2508-2522.